

Subtle White Matter Lesion Detection in Traumatic Brain Injury Using TractSpLearn

Jiqing Huang¹, Yi Chen^{2,3}, Laurent Lamalle¹, Ali Al-Husseini⁴, Anna Gard⁴, Niklas Marklund⁴, Markus Nilsson⁵, Mohamed Ali Bahri¹, Christophe Phillips^{1†}, Evgenios N. Kornaropoulos^{1,5,6*†}

1 GIGA-CRC Human Imaging, University of Liège, Belgium

2 Key Laboratory of Advanced Medical Imaging and Intelligent Computing of Guizhou Province, Guizhou University, China

3 D-Lab, Maastricht University, The Netherlands

4 Department of Clinical Sciences Lund, Neurosurgery, Lund university, Skane University Hospital, Sweden

5 Department of Clinical Sciences Lund, Diagnostic Radiology, Medical Faculty, Lund University, Sweden

6 CRMBM, CNRS, Aix-Marseille University, Marseille, France

Introduction

Traumatic brain injury (TBI) refers to brain damage caused by an external mechanical force, such as a forceful bump, blow, or jolt to the head, or by the penetration of the skull by an object. Patients with TBI may experience persistent cognitive impairments, emotional and behavioural disturbances, and sensory or motor deficits. In severe cases, these issues can lead to long-term disability, with outcomes varying according to the extent, and particularly the location, of the injury.

To detect white-matter lesions in TBI, Attyé et al.¹ introduced TractLearn, a framework that maps patients onto a healthy manifold learned from 3T diffusion tensor imaging (DTI) parametric maps. However, a key limitation is that the framework can still report non-negligible “abnormalities” in healthy controls, indicating residual inter-individual variability and imperfect modelling of the normative distribution.

Building on this concept, the proposed method TractSpLearn explicitly accounts for inter-individual variability to better capture subtle microstructural alterations. In addition, it leverages ultra-high field 7T MRI and a more advanced diffusion kurtosis imaging (DKI) model to improve both sensitivity and specificity.

Method

Participant: This retrospective study validates the performance of TractLearn and TractSpLearn frameworks on a cohort of 56 participants. Ethical approval was obtained from the Institutional Review Board of Lund University, Sweden (Dnr 2017/1049). The cohort comprised 21 healthy non-competing controls, 17

athletes with a history of repeated head injuries (RHI), and 18 athletes with persistent post-concussive syndrome (PPCS). Both structural and diffusion weighted imaging (DWI) were acquired on a 7T Philips Achieva magnetic resonance scanner (T1-weighted imaging: rapid gradient-echo sequence [field of view: $230 \times 230 \times 180$ mm³, resolution: $0.80 \times 0.80 \times 0.80$ mm³, repetition time: 8.00 ms, echo time: 1.97 ms]; DWI [FOV: $224 \times 224 \times 110$ mm³, resolution: $2 \times 2 \times 2$ mm³, TR: 9200 ms, TE = 65 ms, b-value scheme: two b = 0 s/mm² volumes with reversed phase-encoding directions for distortion correction, 6 directions at b = 100 s/mm², 6 directions at b = 500 s/mm², 10 directions at b = 1000 s/mm², and 30 directions at b = 2000 s/mm²]).

Preprocessing and DKI parameters fitting: MR images were pre-processed with a standard pipeline to ensure data quality and consistency across participants². DKI parameters, including fractional anisotropy (FA), mean diffusivity (MD), axial diffusivity (AD), radial diffusivity (RD), mean kurtosis (MK), axial kurtosis (AK), and radial kurtosis (RK), were estimated using weighted linear least squares implemented in DIPY³. These parametric maps were then segmented into a set of white-matter tracts using TractSeg⁴.

TractSpLearn: We implemented a nested cross-validation strategy for unbiased model evaluation, as shown in Fig. 1. The outer loop followed a paired leave-one-out scheme in which each patient–control pair (matched by subject index) was jointly reserved for testing. At the inner level, a k-fold cross-validation (k = 5) was applied to the remaining data for model training and hyperparameter optimization. Within each inner cross-validation loop, both TractLearn and TractSpLearn frameworks were applied independently for each white-matter tract and each DKI parameter. The processing procedure consists of three main steps:

- Features extraction

The manifold features were extracted using UMAP⁵. Unlike the original TractLearn where the manifold features were extracted exclusively from healthy controls, TractSpLearn instead learns shared manifold features from both healthy controls and patients.

- Features projection and back-projection

Tract-wise DKI parameters were first projected to a latent manifold via a forward nonlinear regressor and then reconstructed in the original image space through an inverse mapping. Unlike the original formulation, the mapping is decomposed into a shared baseline and separate components capturing healthy-control inter-individual variability and patient-specific deviations (Fig.1). The bidirectional model is trained and tuned within the inner loop.

- Z-score calculation

In the outer loop, subject-level deviations were quantified using voxel-wise z-scores. For each individual, residuals between original and estimated parameters were standardized by the residual standard deviation estimated from the training healthy controls, enabling direct comparison against the healthy cohort.

Result

Per-subject z-score maps were projected to 2D along the sagittal, coronal, and axial planes to summarize the spatial distribution of tract-related abnormalities. Suprathreshold values were defined as an absolute z-score larger than 4.25 (two-tailed $p \approx 2.1 \times 10^{-5}$) to strongly limit false positives and retain only highly significant deviations. A burden map (b-map) was then computed by counting, for each pixel, how many tracts exceeded this threshold, thereby quantifying the local overlap of abnormal tracts. For each subgroup comparison (RHI vs healthy controls and PPCS vs healthy controls), Fig. 2 presents a representative patient-control pair with the corresponding projected z-score maps and the patient burden map.

Conclusion

Overall, patients showed higher z-scores than healthy controls under both the original and the proposed methods. Across patient subgroups, RHI athletes exhibited more marked abnormalities than PPCS athletes, consistent with a smaller lesion burden and/or partial recovery patterns in PPCS. In addition, the proposed approach provided mean absolute z-score closer to zero in healthy controls-healthy controls and more refined patient-healthy controls contrasts than the original TractLearn. These findings suggest that TractSpLearn improves sensitivity and specificity, although further clinical validation is required.

Acknowledgement

This work was supported by computational resources from the CÉCI (Consortium des Équipements de Calcul Intensif) platform and the SEGI (Service Général de l'Informatique) at the University of Liège (ULiège). We are especially grateful to Prof. David Colignon for his assistance with resource allocation and technical support.

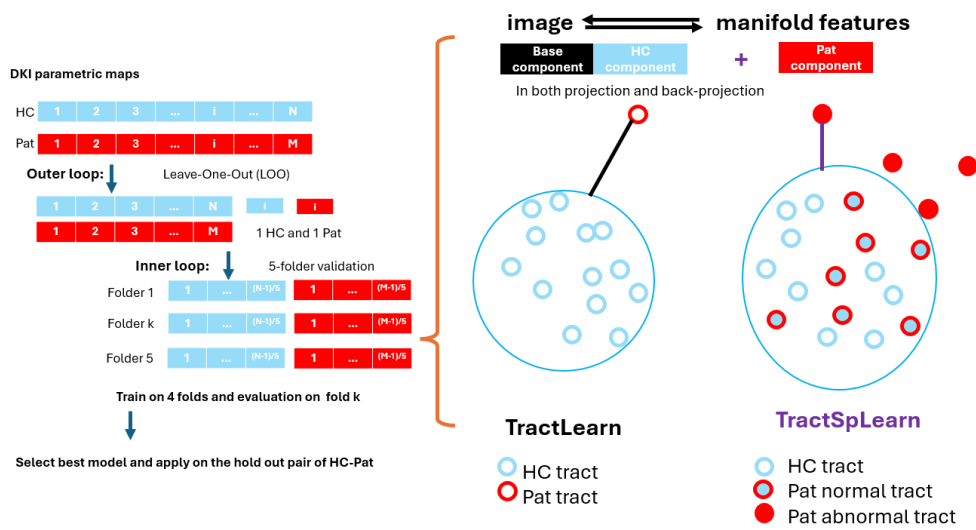


Figure. 1 Flowchart of TractLearn and of TractSpLearn and key differences between TractLearn and TractSpLearn

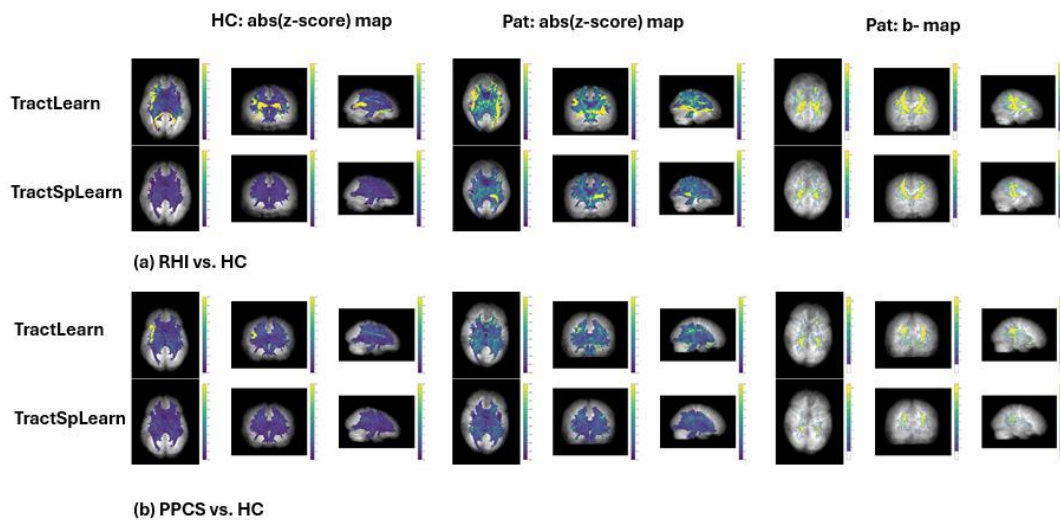


Figure. 2 Mean |z-score| and b-map visualizations for RHI vs healthy controls and PPCS vs healthy controls

Reference

- Attyé A, Renard F, Baciú M, et al. TractLearn: A geodesic learning framework for quantitative analysis of brain bundles. Neuroimage. 2021;233:117927. doi:10.1016/j.neuroimage.2021.117927.

2. Gard A, Kornaropoulos EN, Wernersson MP, et al. Widespread white matter abnormalities in concussed athletes detected by 7T diffusion magnetic resonance imaging. *J Neurotrauma*. 2024;41(13-14):1533-1549. doi:10.1089/neu.2023.0099.
3. Garyfallidis E, Brett M, Amirbekian B, et al. Dipy, a library for the analysis of diffusion MRI data. *Front Neuroinform*. 2014;8:8. doi:10.3389/fninf.2014.00008
4. Wasserthal J, Neher P, Maier-Hein KH. TractSeg - Fast and accurate white matter tract segmentation. *Neuroimage*. 2018;183:239-253. doi:10.1016/j.neuroimage.2018.07.070
5. McInnes L, Healy J, Melville J. UMAP: Uniform Manifold Approximation and Projection for Dimension Reduction. *arXiv*. Published online February 9, 2018. doi:10.48550/arXiv.1802.03426